VIA MEDICA

ORIGINAL ARTICLE

Folia Morphol.
Vol. 67, No. 1, pp. 8–12
Copyright © 2008 Via Medica
ISSN 0015–5659
www.fm.viamedica.pl

The structure of acquired aural cholesteatoma as revealed by scanning electron microscopy

A.J. Miodoński[1], J.A. Litwin[2], J. Składzień[3], K. Zagórska-Świeży[1]

[1]*Laboratory of Scanning Electron Microscopy, Jagiellonian University Medical College, Krakow, Poland*
[2]*Department of Histology, Jagiellonian University Medical College, Krakow, Poland*
[3]*Department of Otorhinolaryngology, Jagiellonian University Medical College, Krakow, Poland*

[Received 12 October 2007; Revised 30 November 2007; Accepted 30 November 2007]

The structural features of cells, their surfaces and the extracellular matrix were investigated in acquired aural cholesteatoma. Cholesteatomas surgically removed from 30 patients were examined by a scanning electron microscope (SEM).
The predominant part of a cholesteatoma was composed of stratified squamous epithelium, showing extensive chaotic desquamation. The surface sculpture of the keratinocytes and corneocytes varied from parallel ridges, irregular microplicae and mirovilli, to flat grooves and pits and a completely smooth surface. Sheet-like lamellar structures, probably representing an intercellular lipid-forming permeability barrier, were also observed. Small crystals located in the perimatrix were observed in one case.
According to the SEM observations, cholesteatoma epithelium is characterised by abnormal and uncoordinated keratinisation, with a predominance of the advanced stages of the process. (Folia Morphol 2008; 67: 8–12)

Key words: epithelium, keratinisation, scanning electron microscopy

INTRODUCTION

Cholesteatoma, a common middle ear disorder, results from abnormal proliferation of the keratinised stratified squamous epithelium which grows into the middle ear, epitympanum or mastoid. Its aetiopathology seems to be multifactorial and includes ingrowth of the epithelium into a retraction pocket of the tympanic membrane, epithelial migration, tympanic perforation, local epithelial hyperplasia or even squamous cell metaplasia of the middle ear epithelium with possible involvement of the papillomavirus [3, 11].

Proliferation and centripetal accumulation of keratinocytes is responsible for the characteristic histology of cholesteatoma, in which three distinct zones can be distinguished. The most peripheral zone, the perimatrix, originates from the lamina propria of the middle ear mucosa and shows the features of inflamed connective tissue or granulation tissue [8, 10]. Proliferating stratified squamous epithelium forms the matrix, and desquamated corneocytes accumulating in the central area of the lesion have been termed the cystic content.

The growth of cholesteatoma results from an imbalance between two opposite processes, namely the proliferation and apoptosis of keratinocytes. As compared with meatal skin, both the proliferative index and the apoptotic index have been found to be higher in cholesteatoma [2, 6, 7, 9], but it seems that the increased proliferation of keratinocytes is not sufficiently counteracted by increased apoptosis.

The structure of cholesteatomas was investigated in detail by transmission electron microscopy [5]. In the matrix, the authors observed all the layers typical for normal epidermis as well as Langerhans

Address for correspondence: Prof. J.A. Litwin, Department of Histology, Jagiellonian University Medical College, Kopernika 7, 31–034 Krakow, Poland, tel: +48 12 422 70 27, fax: +48 12 422 70 27, e-mail: mmlitwin@cyf-kr.edu.pl

cells. The perimatrix contained collagen fibres, fibroblasts and inflammatory cells. However, there are very few papers that present observations of cholesteatoma in the scanning electron microscope (SEM) [8, 12, 17] and the observations that have been reported are often fragmentary. The aim of the present study, therefore, was to examine surgically removed cholesteatomas by SEM.

MATERIAL AND METHODS

The material consisted of 30 acquired aural cholesteatomas removed surgically from patients (20 men, 10 women, aged 18–75 years, mean age 36 years) at the Department of Otorhinolaryngology, Jagiellonian University Medical College, in the period 2002–2003. In the investigated material 9 cholesteatomas had been diagnosed as primary, 11 as secondary and 10 as uncertain. The cholesteatomas were located in the anterior mesotympanum, posterior mesotympanum or in the mastoid area.

After surgery the cholesteatomas were gently washed in saline and halved, each half then being used for histopathological and SEM examination respectively.

For routine light microscopic histopathology the specimens were fixed in 10% buffered formalin, embedded in paraffin, sectioned and stained with haematoxylin-eosin.

For SEM, the specimens were processed according to protocol 3 of Toskala [16], guaranteeing the lowest incidence of artefacts. They were fixed in 1% paraformaldehyde/1.23% glutaraldehyde in 0.2 M cacodylate buffer, pH 7.3 for 24 hours at 4°C, thoroughly washed several times in the same buffer and postfixed in 2% osmium tetroxide for three hours. After dehydration in a graded series of ethanol followed by absolute acetone, the samples were critical-point dried in CO_2, coated with carbon and gold and examined in a Jeol JSM 35 CF SEM at 25 kV.

RESULTS

The diagnosis of the surgically removed cholesteatomas was in all cases confirmed by routine histopathology. The outer surface of the cholesteatomas examined in SEM revealed the presence of partially preserved perimatrix and an outer surface of matrix (Fig. 1). The appearance of the perimatrix differed in individual cases; sometimes it was very rich in cells, suggesting an inflammatory process (Fig. 2), but otherwise it contained collagen strands and interspersed mononuclear cells with stubby microvilli (lymphocytes, macrophages, neutrophils), as well as occasional red blood cells (Fig. 3).

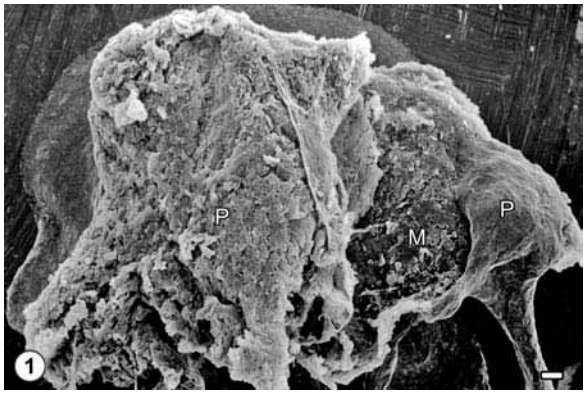


Figure 1. Low power view of surgically removed cholesteatoma showing incomplete perimatrix (P) and areas of exposed matrix (M). Bar = 100 μm.

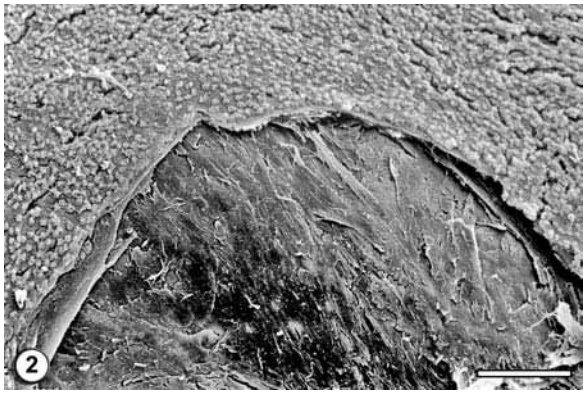


Figure 2. Perimatrix characterised by very high cell density. Bar = 100 μm.

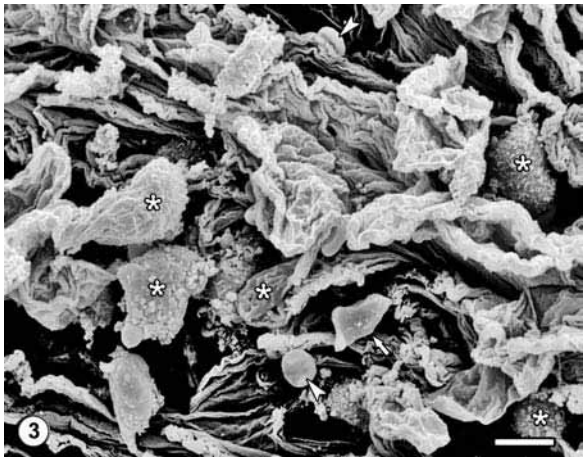


Figure 3. An area of perimatrix with collagen strands, migratory cells (asterisks) and a few erythrocytes (arrowheads). Note a small crystal (arrow) present in the perimatrix. Bar = 10 μm.

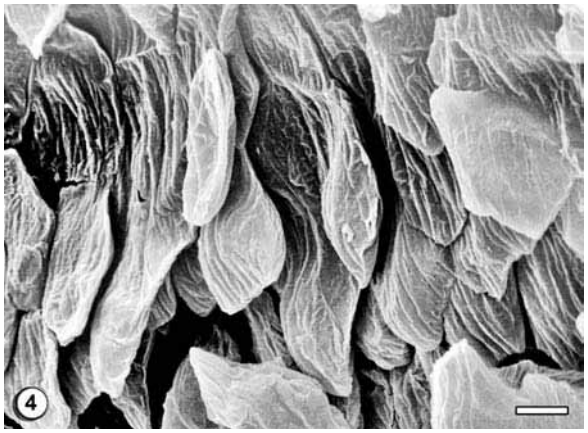


Figure 4. Polygonal cells of the matrix with prominent parallel ridges on the surface. Bar = 10 μm.

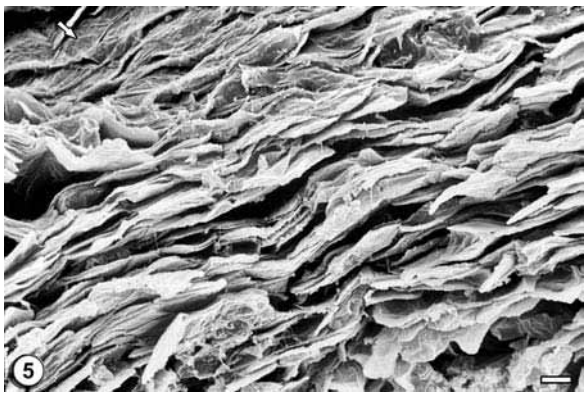


Figure 5. Squamous keratinocytes of the matrix, showing unordered stacking pattern and irregular microplicae on the surface (arrow). Bar = 10 μm.

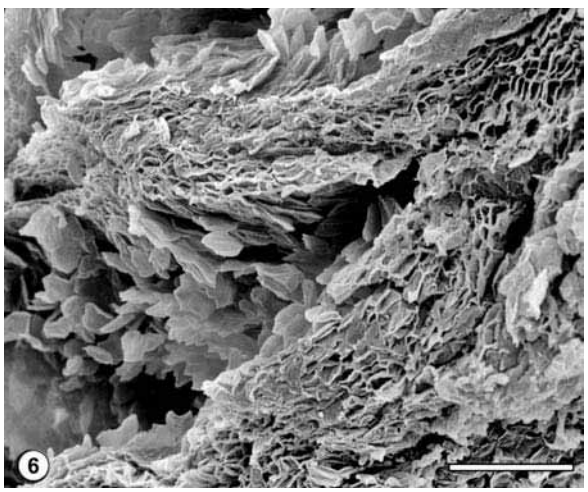


Figure 6. Chaotic desquamation of large corneocyte clusters in the cystic part. Bar = 100 μm.

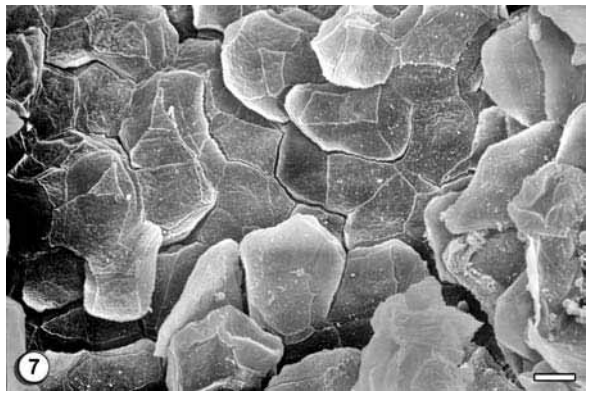


Figure 7. A border zone between the matrix and the cystic part. Note a gradual transition of corneocyte surface sculpture from irregular flat microplicae (left), shallow grooves and pits (middle) to completely smooth surface (right). Bar = 10 μm.

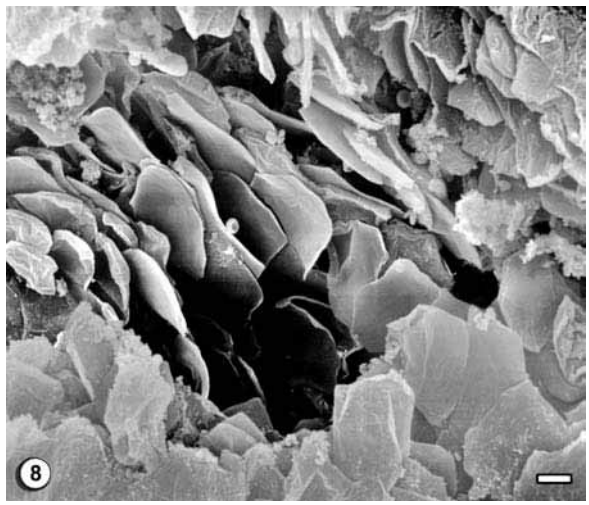


Figure 8. Focal corneocyte desquamation in the cystic part. Some corneocytes have shallow grooves and pits on their surface, while the others are completely smooth and resemble plate-like crystals. Bar = 10 μm.

The deeper layers of the matrix exposed after cutting the cholesteatoma into halves were composed of polygonal cells with prominent parallel surface ridges (Fig. 4). The predominant part of the matrix was composed of multiple layers of stacked sqamous cells with irregular flat microplicae and microvilli on their surface. The intercellular spaces were dilated and twisted (Fig. 5). In the cystic content these cells were already transformed into corneocytes (anuclear keratin squames). This area showed extensive desquamation of large corneocyte clusters, often resulting in a chaotic orientation of desquamated cells (Fig. 6). The surface of some desquamated corneocytes showed the presence of shallow grooves and pits, while in others it was completely smooth, so that such keratin squames resembled plate-like crystals (Figs. 7, 8).

In the matrix zone, including the spinous layer and its transition into the keratinised layer,

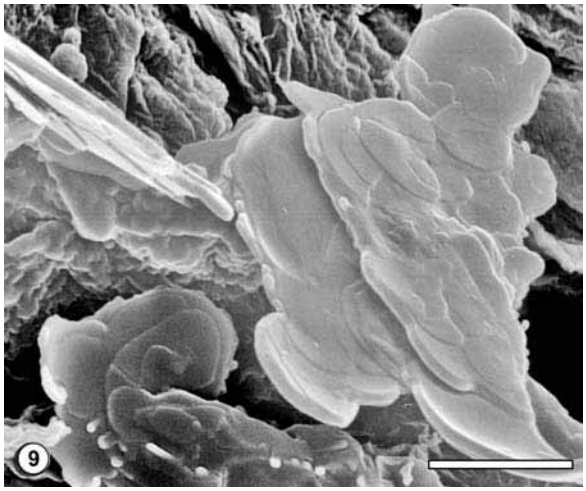


Figure 9. Sheet-like smooth structure with laminar appearance (probably lipid layer) between matrix cells. Bar = 10 μm.

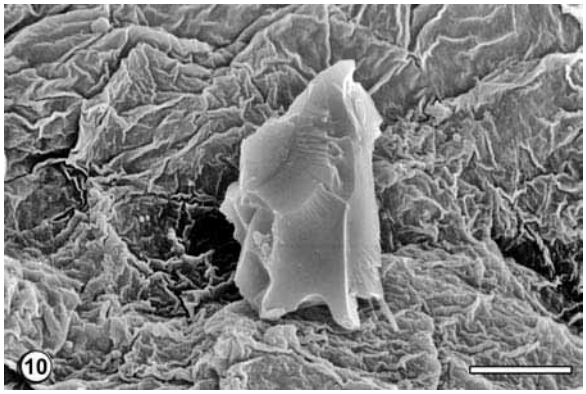


Figure 10. A crystal located on the basal surface of the matrix. Bar = 10 μm.

smooth sheet-like structures with rounded contours and lamellar appearance were observed between cells in some of the places exposed after cutting (Fig. 9).

In one out of 30 examined cases a few small crystals, probably of cholesterol, were found at the interface between the perimatrix and the matrix (Fig. 10).

The structural characteristics of the cholesteatomas revealed by SEM were the same, irrespective of cholesteatoma location or character (whether primary or secondary).

DISCUSSION

The predominant feature of cholesteatoma observed in the SEM was a massive chaotic desquamation of corneocytes. In our material we have never observed a regular stacking pattern of squamous keratinocytes, as reported by Youngs and Rowles [17] in their SEM study. This suggests that the proliferation of keratinocytes in cholesteatoma is much less coordinated as compared with normal epidermis, in which such a stacking pattern is typical.

We were unable to observe the variable surface sculpture pattern of squamous keratinocytes described by us previously in aural polyps with underlying cholesteatoma [13]: prominent microvilli, complex microplicae or borderline microplicae. Instead, the surface of the keratinocytes showed parallel ridges, flat irregular microplicae accompanied by short microvilli, irregular shallow grooves and pits or a completely smooth surface. Such surface features suggest abnormal keratinisation and the predominance of cells at advanced stages of the process. A completely smooth corneocyte surface is very rarely observed; this probably corresponds to the very terminal stage of keratinisation achieved by corneocytes during their long-term accumulation in the central area of cholesteatoma. Such smooth corneocytes viewed in SEM could even be erroneously interpreted as plate-like cholesterol crystals, which may be very similar in appearance [1, 13].

The smooth sheet-like structures observed between keratinocytes have not yet been described in cholesteatoma. They probably represent the intercellular lipid layers described by Svane-Knudsen et al. [14, 15], which form the permeability barrier in the epithelium. Our SEM observations correspond to the findings of the last-mentioned authors, who reported discontinuity of the lipid sheets accompanied by large dilatations of the intercellular spaces in the stratum corneum and suggested that the permeability barrier might be defective in cholesteatoma [15].

Generally, in contrast to cholesterol granuloma, cholesteatoma does not contain cholesterol crystals [4]. Single crystals or characteristic "cholesterol clefts" can, however, occasionally be found in the perimatrix [10]. We observed a few irregular crystals only in one out of 30 examined cases.

In summary, according to our SEM observations, the cholesteatoma epithelium is characterised by abnormal and uncoordinated keratinisation, with a predominance of the advanced stages of the process.

REFERENCES

1. Busch N, Lammert F, Marschall HU, Matern S (1995) A new subgroup of lectin-bound biliary proteins binds to cholesterol crystals, modifies crystal morphology, and inhibits cholesterol crystallization. J Clin Invest, 96: 3009–3015.

2. Ergun S, Carlsoo B, Zheng X (1999) Apoptosis in meatal skin, cholesteatoma and squamous cell carcinoma of the ear. Clin Otolaryngol Allied Sci, 24: 280–285.
3. Ferekidis E, Nikolopoulos TP, Yiotakis J, Ferekidou E, Kandiloros D, Papadimitriou K, Tzangaroulakis A (2006) Correlation of clinical and surgical findings to histological features (koilocytosis, papillary hyperplasia) suggesting papillomavirus involvement in the pathogenesis of cholesteatoma. Med Sci Monit, 12: CR368–CR371.
4. Ferlito A, Devaney KO, Rinaldo A, Milroy CM, Wenig BM, Iurato S, McCabe BF (1997) Clinicopathological consultation. Ear cholesteatoma versus cholesterol granuloma. Ann Otol Rhinol Laryngol, 106: 79–85.
5. Lim DJ, Saunders WH (1972) Acquired cholesteatoma: light and electron microscopic observations. Ann Otol Rhinol Laryngol, 81: 1–11.
6. Olszewska E, Chodynicki S, Chyczewski L (2006) Apoptosis in the pathogenesis of cholesteatoma in adults. Eur Arch Otorhinolaryngol, 263: 409–413.
7. Olszewska E, Chodynicki S, Chyczewski L, Rogowski M (2006) Some markers of proliferative activity in cholesteatoma epithelium in adults. Med Sci Monit, 12: CR337–CR340.
8. Paludetti G, Almadori G, Ottaviani F, Rosignoli M, Rossodivita M, D'Alatri L (1989) Ultrastructural aspects of cholesteatoma of the middle ear. Acta Otorhinolaryngol Ital, 9: 169–180.
9. Pereira CSB, Almeida CIR, Vianna MR (2002) Immunoexpression of cytokeratin 16 and Ki-67 nuclear antigen in acquired cholesteatoma of middle ear. Rev Bras Otorinolaringol, 68: 453–460.
10. Schaper J, van de Heyning J (1976) Cholesteatoma of the middle ear in human patients. An ultrastructural study. Arch Otolaryngol, 102: 663–668.
11. Semaan MT, Megerian CA. The pathophysiology of cholesteatoma (2006) Otolaryngol Clin North Am, 39: 1143–1159.
12. Shimooka R, Yajin K, Harada Y (1983) SEM studies of the inflammatory changes of the middle ear mucosa. Auris Nasus Larynx, 10: 79–86.
13. Składzień J, Litwin JA, Nowogrodzka-Zagórska M, Miodoński AJ (2002) Surface structures of aural polyps: a scanning electron microscopic study. J Laryngol Otol, 116: 420–425.
14. Svane-Knudsen V, Halkier-Sorensen L, Rasmussen G, Ottosen PD (2001) Cholesteatoma: a morphologic study of stratum corneum lipids. Acta Otolaryngol, 121: 602–606.
15. Svane-Knudsen V, Halkier-Sorensen L, Rasmussen G, Ottosen PD (2002) Altered permeability barrier structure in cholesteatoma matrix. Eur Arch Otorhinolaryngol, 259: 527–530.
16. Toskala E (1995) The influence of specimen preparation on artefacts in scanning electron microscopy of respiratory cilia. Biotechnol Histochem, 70: 46–51.
17. Youngs R, Rowles P (1990) The spatial organisation of keratinocytes in acquired middle ear cholesteatoma resembles that of external auditory canal skin and pars flaccida. Acta Otolaryngol, 110: 115–119.